AFRL-RZ-WP-TP-2010-2247

HIFiRE FLIGHT 2 FLOWPATH DESIGN UPDATE (PREPRINT)

Mark R. Gruber

Propulsion Sciences Branch
Aerospace Propulsion Division

Paul Ferlemann and Keith McDaniel

NASA Langley Research Center

DECEMBER 2009

AIR FORCE RESEARCH LABORATORY
PROPULSION DIRECTORATE
WRIGHT-PATTERSON AIR FORCE BASE, OH 45433-7251
AIR FORCE MATERIEL COMMAND
UNITED STATES AIR FORCE

REPORT DOCUMENTATION PAGE

Form Approved
OMB No. 0704-0188

1. REPORT DATE *(DD-MM-YY)*	2. REPORT TYPE	3. DATES COVERED *(From - To)*
December 2009	Conference Paper Preprint	01 August 2008 – 01 November 2009

4. TITLE AND SUBTITLE
HIFiRE FLIGHT 2 FLOWPATH DESIGN UPDATE (PREPRINT)

5a. CONTRACT NUMBER
In-house

5b. GRANT NUMBER

5c. PROGRAM ELEMENT NUMBER
62203F

6. AUTHOR(S)
Mark R. Gruber (AFRL/RZAS)
Paul Ferlemann and Keith McDaniel (NASA Langley Research Center)

5d. PROJECT NUMBER
3012

5e. TASK NUMBER
AI

5f. WORK UNIT NUMBER
3012AI00

7. PERFORMING ORGANIZATION NAME(S) AND ADDRESS(ES)
Propulsion Sciences Branch (AFRL/RZAS)
Aerospace Propulsion Division
Air Force Research Laboratory, Propulsion Directorate
Wright-Patterson Air Force Base, OH 45433-7251
Air Force Materiel Command, United States Air Force

NASA Langley Research Center
ATK Space Division
Hampton, VA 23681

8. PERFORMING ORGANIZATION REPORT NUMBER
AFRL-RZ-WP-TP-2010-2247

9. SPONSORING/MONITORING AGENCY NAME(S) AND ADDRESS(ES)
Air Force Research Laboratory
Propulsion Directorate
Wright-Patterson Air Force Base, OH 45433-7251
Air Force Materiel Command
United States Air Force

10. SPONSORING/MONITORING AGENCY ACRONYM(S)
AFRL/RZAS

11. SPONSORING/MONITORING AGENCY REPORT NUMBER(S)
AFRL-RZ-WP-TP-2010-2247

12. DISTRIBUTION/AVAILABILITY STATEMENT
Approved for public release; distribution unlimited.

13. SUPPLEMENTARY NOTES
Paper presented at the JANNAF Joint Subcommittee Meeting, meeting held December 7 - 11, 2009 in San Diego, CA. This paper contains color. PA Case Number: 88ABW 2009-4771; Clearance Date: 18 Nov 2009.

14. ABSTRACT
This paper describes the evolution of various aspects of the flowpath design as the payload system design has matured. Forebody design changes were required in order to reduce the overall payload system weight and to meet shroud design requirements. In response to the forebody design changes, modifications were made to the fuel injectors within the combustor as the captured air mass flow rate reduced. No additional changes were made to the isolator/combustor relative to the baseline flowpath. Forebody design changes allowed the nozzle design to be adjusted resulting in additional payload weight and length reductions. Finally, in an attempt to mitigate any adverse effects during the boost phase of the flight trajectory, stationary covers were designed to protect the scramjet nozzle exit regions. Each of these modifications will be described in this paper along with relevant analysis results to illustrate the effects on the overall payload system. The updated instrumentation plan for the current payload system will also be described.

15. SUBJECT TERMS
supersonic combustion, scramjet, fuel injection, flameholding

16. SECURITY CLASSIFICATION OF:			17. LIMITATION OF ABSTRACT:	18. NUMBER OF PAGES	19a. NAME OF RESPONSIBLE PERSON (Monitor)
a. REPORT	b. ABSTRACT	c. THIS PAGE			Mark R. Gruber
Unclassified	Unclassified	Unclassified	SAR	22	19b. TELEPHONE NUMBER *(Include Area Code)* N/A

Standard Form 298 (Rev. 8-98)
Prescribed by ANSI Std. Z39-18

HIFIRE FLIGHT 2 FLOWPATH DESIGN UPDATE

Mark Gruber*
Air Force Research Laboratory
Propulsion Directorate
Wright-Patterson AFB, OH 45433

Paul Ferlemann† and Keith McDaniel†
ATK Space Division
NASA Langley Research Center
Hampton, VA 23681

ABSTRACT

The HIFiRE Flight 2 experiment aims to study mode transition and supersonic combustion performance using a surrogate hydrocarbon fuel over a Mach number range from 5.5 to 8+. The experiment will use a sounding rocket stack and a novel second-stage ignition approach to achieve a nearly constant flight dynamic pressure over this range of Mach numbers. The experimental payload will remain attached to the second-stage rocket motor and the experiment will occur while accelerating through the atmosphere. The scramjet flowpath (forebody, inlet, isolator, combustor, and nozzle) will be heavily instrumented, using both conventional wall instrumentation and in-stream optical diagnostics, in order to adequately assess the operability and performance of the device as well as verify the tools used for its design. This paper describes the evolution of various aspects of the flowpath design as the payload system design has matured. Specifically, forebody design changes were required in order to reduce the overall payload system weight and to meet shroud design requirements. In response to the forebody design changes, modifications were made to the fuel injectors within the combustor as the captured air mass flow rate reduced. No additional changes were made to the isolator/combustor relative to the baseline flowpath. Forebody design changes allowed the nozzle design to be adjusted resulting in additional payload weight and length reductions. Finally, in an attempt to mitigate any adverse effects during the boost phase of the flight trajectory, stationary covers were designed to protect the scramjet nozzle exit regions. Each of these modifications will be described in this paper along with relevant analysis results to illustrate the effects on the overall payload system. The updated instrumentation plan for the current payload system will also be described.

NOMENCLATURE

A	=	area
C_d	=	discharge coefficient
C_f	=	skin friction coefficient
C_p	=	specific heat at constant pressure
d	=	fuel injector diameter
$(f/a)_{ST}$	=	stoichiometric fuel-air ratio
k	=	turbulent kinetic energy
M	=	Mach number
P	=	pressure
q	=	dynamic pressure
ST	=	stream thrust
T	=	temperature
V	=	velocity
W	=	mass flow rate
x,y,z	=	axial, transverse, and spanwise coordinates
Z	=	altitude
ϕ	=	equivalence ratio

* Principal Aerospace Engineer.
† Aeronautical Engineer.

ϕ_B = burned equivalence ratio = $\phi * \eta_c$
γ = specific heat ratio
η_c = combustion efficiency
η_{KE} = kinetic energy efficiency
ρ = density

Subscripts
air = air stream
f = fuel stream
t = total or stagnation condition
4 = combustor exit station
9 = 9-inch capture height
12 = 12-inch capture height

INTRODUCTION

The Hypersonic International Flight Research Experimentation (HIFiRE) Program is a joint effort between the US Air Force Research Laboratory (AFRL) and the Australian Defence Scientific and Technology Organisation (DSTO) devoted to the study of basic hypersonic phenomena through flight experimentation. As part of this multi-flight program, the HIFiRE Flight 2 (HF2) Project has been planned to explore the operating, performance, and stability characteristics of a simple hydrocarbon-fueled scramjet combustor as it transitions from dual-mode to scramjet-mode operation and during supersonic combustion at Mach 8+ flight conditions.[1] Objectives of the HF2 flight experiment include:

- Evaluate engine performance and operability through a dual-mode to scramjet-mode transition.
- Achieve Mach 8 combustion performance of $\phi_{B,4} \geq 0.7$ using a hydrocarbon fuel.
- Evaluate a gaseous fuel mixture as a surrogate for cracked liquid hydrocarbon fuel.
- Provide a test bed for diode laser-based instrumentation (water vapor and perhaps oxygen).
- Validate existing design tools for scramjet inlet, isolator, combustor, and nozzle components.
- Demonstrate a flight test approach that provides a variable Mach number flight corridor at nearly constant dynamic pressure.

During the payload conceptual design process, a baseline flowpath design was sufficiently matured to allow weight and drag estimates necessary for trajectory analyses to be conducted using candidate rocket motors. The preliminary trajectory analyses indicated that the required maximum Mach number could not be achieved using the specified boosters. In addition, the requirements for the forebody shroud associated with the baseline payload design were beyond the experience base of the shroud manufacturer. Together, these results dictated that a payload design change be made to reduce overall payload weight, length, and diameter.

This paper describes the approach to and results of modifying the HF2 flowpath design in order to address these issues while maintaining the ability to achieve the experimental objectives. First, the forebody capture height was adjusted such that overall payload diameter and length could be reduced. This change resulted in reduced air mass capture, which necessitated a change in fuel injector size. The resized forebody also enabled the nozzle section to be significantly shortened. Nozzle exit covers were added in an attempt to protect the nozzle exit regions from the adverse thermal environment. Finally, the instrumentation layout was modified in response to these flowpath changes. Each of these topics will be described in the following sections.

FOREBODY/INLET DESIGN MODIFICATIONS

The original forebody/inlet for HF2 was designed to meet program requirements, provide high quality flow (low distortion and low sensitivity to angle of attack and sideslip) to the combustor, and be

conservative for inlet starting.[2] However, additional weight and shroud size constraints were imposed which required a smaller forebody design. Therefore, the forebody capture height was reduced from 12- to 9-inches. The reduction in external compression made the design more conservative with respect to inlet starting by increasing the one-dimensional inlet entrance Mach number for flight at Mach 5 from 2.26 to 2.44, with Kantrowitz[3] internal contraction ratios of 1.27 and 1.31 (current design has a value of 1.2). This section documents the computational approach and results from simulations of the smaller design.

GEOMETRY DEFINITION

The geometry used to create the grid for high-resolution forebody and inlet analysis was created in Gridgen (see Figure 1). The grid was generated before the final geometry was created. Thus, exterior surfaces of the forebody are different from the final design geometry, but the internal flowpath is identical to the final design geometry. The flowpath has 0.030-inch radius leading edges with a capture height of 9-inches measured from the bluntness interior tangency points. The nose (cylindrical part) is 4.5-inches wide. Each forebody surface generates 7-deg. of compression. Each chine begins at (x, z)=(20.94, 7.28) and progresses at 19.8-deg. to the inlet entrance at (x, z)=(32.806,3). This allows for 5-deg. of margin from the local wave angle for flight at Mach 5 (Mach 3.87 produces a wave angle of 15-deg.). Therefore, the relief provided by the chines will not affect the captured flow. The inlet entrance is 4.8-inches wide measured from the interior tangency point of the 0.030-inch radius blunt inlet sidewall leading edges. Each inlet sidewall produces 3-deg. of compression and requires 7.63-inches of streamwise length to produce the final flowpath width of 4-inches. The payload diameter is 16-inches at the end of the chines.

GRID GENERATION

Block boundaries from the high-resolution forebody and inlet grid are shown in Figure 1. The forebody was divided into two pieces; nose and ramp. This was done to change the physical model; the nose was laminar and the ramp turbulent. The boundary layer trip strip was not explicitly modeled, but was assumed to be effective. The inlet and isolator were modeled as a third section. Tecplot was used to interpolate the flow between the nose and ramp, and between the ramp and inlet, due to a change in the number of points in the vertical and horizontal directions. The ramp section ended at the forebody exit and no grid was generated for the remainder of the chine or spillway since it was not needed for propulsion analysis. The computational cells were distributed as follows:

- Nose: 4,018,176
- Ramp: 7,147,520
- Inlet/isolator: 9,630,720

The wall clustering was from 5E-5 to 1E-4 inches to maintain a y+ of approximately 1 or less. The streamwise cell size on the ramp surface was 0.02-inches. The inlet entrance was resolved with 80 cells vertically and 152 cells horizontally.

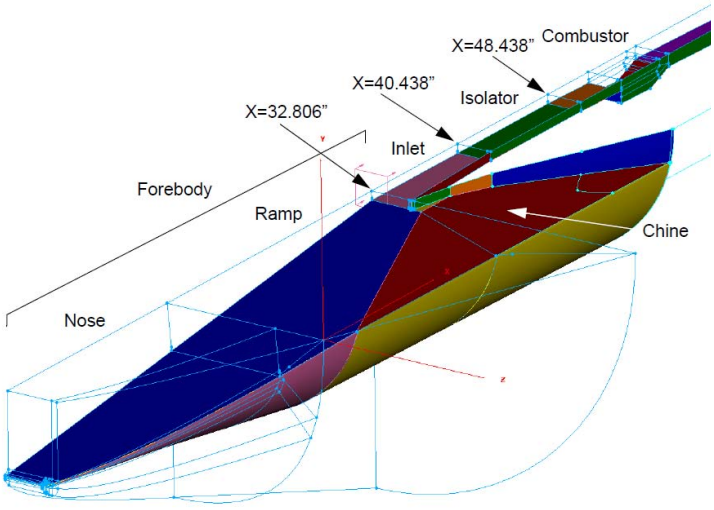

Figure 1. Block structure created in Gridgen for propulsion analysis (1/4 of full geometry).

COMPUTATIONAL APPROACH

The VULCAN CFD software (version 6.0.1)[4] was used to compute the flowfield. The air was modeled as thermally perfect. All solid boundaries were modeled as isothermal with increasing surface temperature at higher Mach numbers. The k-omega turbulence model was activated 15-inches from the nose leading edge (location of boundary

Table 1. Freestream conditions and assumed surface temperature.

M	q		Z	ρ	P	T	V	Wall Temperature (K)		
	(psf)	(kPa)	(m)	(kg/m3)	(Pa)	(K)	(m/s)	Nose	Ramp	Inlet
5.0	2000	95.76	20066	0.08801	5472.1	216.7	1475	300	300	300
6.0	1817	87.00	23027	0.05478	3452.3	219.6	1782		400	600
7.0	1730	82.83	25353	0.03792	2415.0	221.9	2090			700
8.0	1600	76.61	27626	0.02658	1710.0	224.2	2401		500	800
8.5	1000	47.89	31576	0.01446	946.7	2281	2573	400	600	

layer trip strip) and integrated to the wall. Three levels of grid sequencing were used along with the LDFSS solver and DAF scheme. A second-order flux reconstruction was used on each fine grid with the smooth limiter. At an angle of attack and sideslip of zero, one quarter of the full geometry was modeled. Freestream conditions from the nominal trajectory (Mach 5 – 8) and surface temperature distribution are listed in Table 1. An off-nominal set of conditions was also studied at Mach 8.5. This represents an extreme condition, but one that corresponds to a corner of the acceptable test box within the atmosphere.

ANALYSIS RESULTS

Various analysis results will be presented in this section including centerline Mach number contours, surface pressure contours, cross-flow plane Mach number distributions, and one-dimensional properties. Together, these results reveal that the modified forebody geometry provides acceptable flow quality and performance over the anticipated range of flight conditions. The new design does not, however, meet the original throat static pressure requirement at the Mach 8.5, q = 1000 psf condition. This exception was deemed acceptable and the modified forebody design was summarily adopted.

Centerline Mach Number Contours

Contours of Mach number along the spanwise centerline are shown in Figure 2 for the nominal trajectory conditions. These plots reveal the effect of shallower shock wave angles as the Mach number increases.

Surface Pressure Distributions

Contour plots of surface pressure are shown in Figure 3 for each Mach number along the nominal trajectory. Note that a logarithmic scale has been used to emphasize relatively small pressure differences

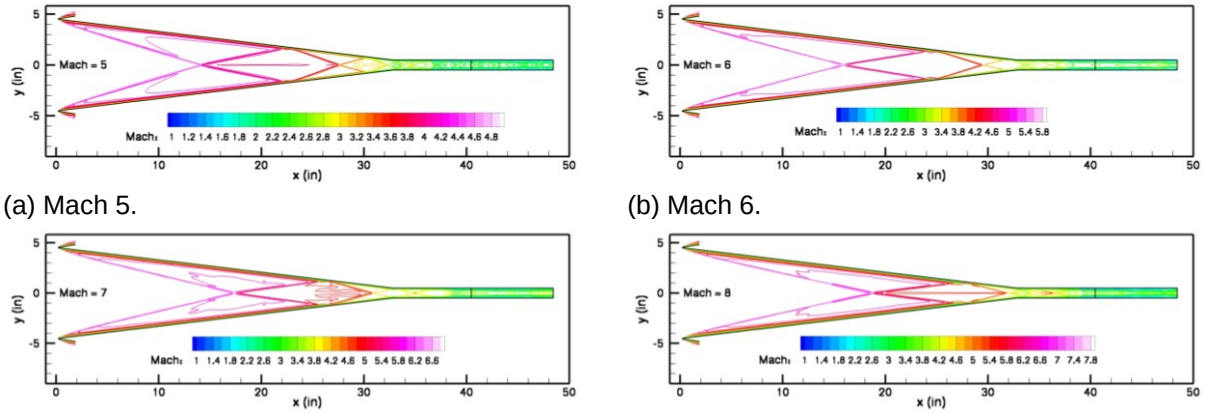

(a) Mach 5. (b) Mach 6.

(c) Mach 7. (d) Mach 8.

Figure 2. Centerline Mach contours.

on the forebody. The contours indicate the curved nature of the first shock reflection and relief provided by the chines. Four surface streamlines are also included. One is approximately at 1/4 of the inlet entrance width. The second represents the surface captured streamline. The remaining two outboard surface streamlines demonstrate that the increasing forebody width and slightly higher pressure along the outboard rim are effective in keeping the flow aligned and minimizing lateral spillage. The angle of the captured streamline is created near the nose but then maintained for the remainder of the forebody.

Heat flux and shear stress results were also examined to assess magnitudes of peak heat flux and regions having the potential for boundary layer separation. With respect to heat flux on flowpath surfaces (excluding the blunt leading edges), the results indicate that the highest magnitudes are found in regions off the spanwise centerline in the inlet and isolator at Mach 8 even though these regions were modeled with the highest surface temperatures. The peak heat flux levels for each case were (BTU/in^{2}s): Mach 5 = 1.4, Mach 6 = 1.2, Mach 7 = 2.0, Mach 8 = 2.5. The results also indicate that no boundary layer separation is predicted to occur on the forebody or along the centerline of the inlet and isolator. Small regions of separated flow are possible near the inlet sidewall leading edge at every Mach number.

Isolator Exit Mach Number Contours

Mach number contours at the isolator exit plane (x = 48.438-inches) are shown in Figure 4 for tare conditions at each flight Mach number along the nominal trajectory. In each case the lowest contour level is 1 with any subsonic areas left unshaded. The subsonic regions for all cases are extremely small. The boundary layers are fairly uniform laterally, except at Mach 8 where the boundary layer thickens at the centerline and at 1.1-inches laterally by the end of the isolator.

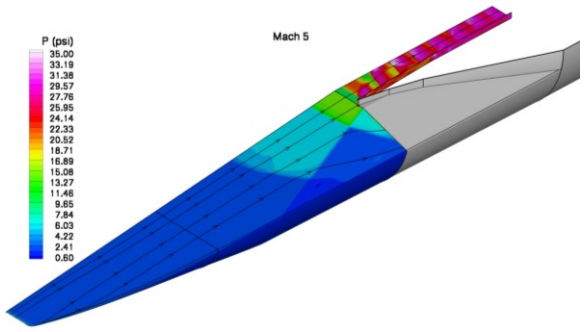

(a) Mach 5.

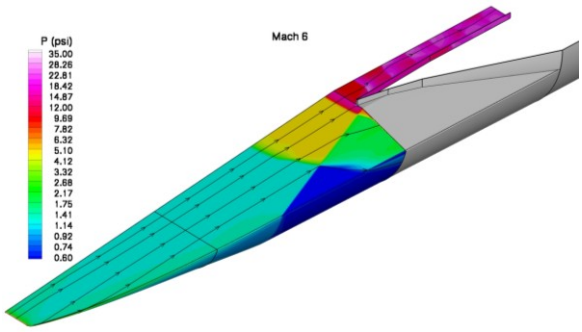

(b) Mach 6.

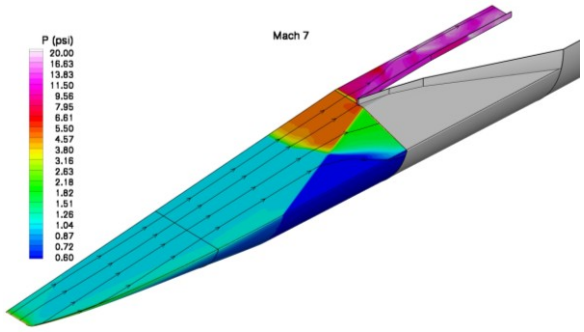

(c) Mach 7.

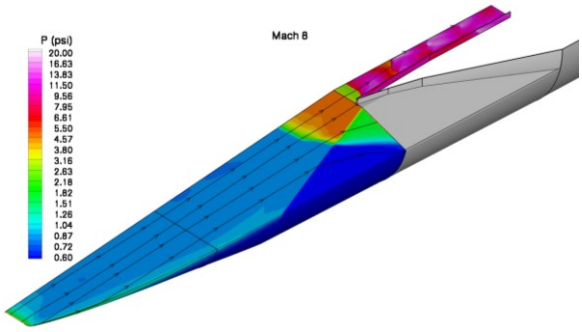

(d) Mach 8.

Figure 3. Surface pressure results.

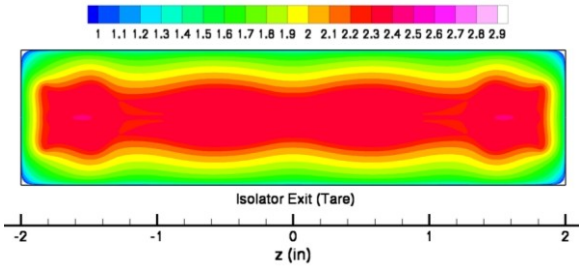

(a) Mach 5.

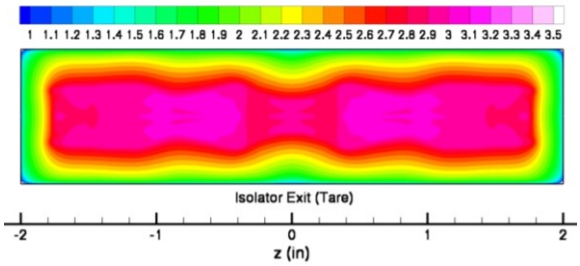

(b) Mach 6.

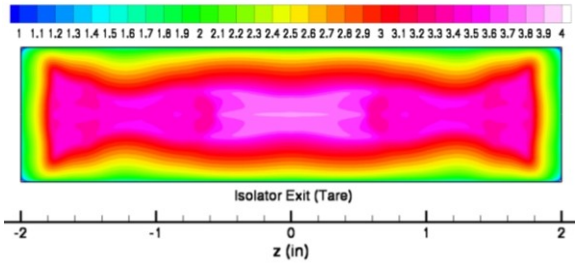

(c) Mach 7.

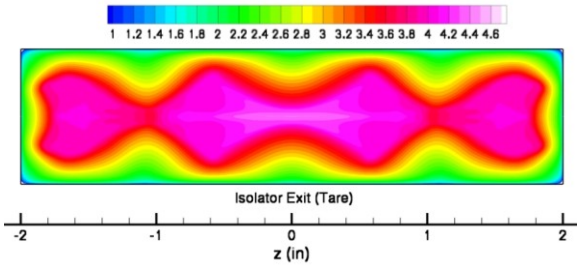

(d) Mach 8.

Figure 4. Crossflow Mach number contours at the isolator exit plane.

One-Dimensional Flow Properties

Table 2 contains the mass capture schedule for the revised forebody design. The mass capture is approximately 80% of the original design. This occurs, even though 9/12 = 0.75, because the amount of lateral spillage decreases in the revised design. The reference area for calculating the spillage percentage was 9 x 4.8 inches.

Table 2. Inlet mass capture.

Flight Mach Number	q		Spillage (%)	W_{air}	
	(psf)	(kPa)		(lbm/s)	(kg/s)
5.0	2000	95.76	24.0	6.07	2.75
6.0	1817	87.00	19.9	4.81	2.18
7.0	1730	82.83	17.1	4.03	1.83
8.0	1600	76.61	15.7	3.32	1.50
8.5	1000	47.89	14.8	1.95	0.88

Properties at the inlet entrance and the isolator exit are listed in Table 3 and Table 4, respectively. The 1D inlet entrance Mach number is approximately half of the freestream Mach number. Along the nominal dynamic pressure trajectory the minimum isolator exit pressure occurs at Mach 8 and remains more than 50% above the original 1/2 atmosphere minimum pressure requirement[2] (1/2 atm = 7.35 psi = 50.66 kPa). The isolator exit pressure predicted for the Mach 8.5 condition falls 5% below the original requirement.

FOREBODY/INLET INSTRUMENTATION PLAN

A total of 77 pressure taps and 48 thermocouples are planned to be integrated into the forebody and inlet sections. Two Pitot pressure measurements (one in each forebody leading edge) are included in this plan. The majority of the pressure taps are positioned on the spanwise centerline of the flowpath, although off-centerline measurements will be made at several axial stations. There is a high degree of body-to-cowl symmetry in the instrumentation plan, but the cowl wall has regions which are more densely instrumented. Wall temperatures are included in a similar fashion. Figure 5 illustrates the current

Table 3. Inlet entrance properties.

Flow Property	Mach 5.0 q 2000 psf	Mach 6.0 q 1817 psf	Mach 7.0 q 1730 psf	Mach 8.0 q 1600 psf
CL wall shear (Pa)	1228	1572	880	996
C_f (1D)	0.0023	0.0030	0.0016	0.0019
ST (N)	3611	3538	3538	3359
ρ (kg/m^3)	0.759	0.468	0.323	0.228
V (m/s)	1175	1507	1830	2136
M	2.44	3.01	3.53	3.93
P_t (kPa)	2059	3527	6060	8883
P (kPa)	127.9	85.35	63.43	49.64
T_t (K)	1206	1620	2095	2635
T(K)	588	635	684	758
γ	1.377	1.372	1.367	1.358
C_p (J/kg-K)	1048	1058	1070	1088
η_{KE}	0.9523	0.9527	0.9540	0.9516
η_{KE} (adiabatic)	0.9715	0.9707	0.9713	0.9696
Total Pressure Recovery	0.659	0.539	0.451	0.349

Table 4. Isolator exit properties (tare conditions).

Flow Property	Mach 5.0 q 2000 psf	Mach 6.0 q 1817 psf	Mach 7.0 q 1730 psf	Mach 8.0 q 1600 psf
CL wall shear (Pa)	1453	1161	1149	1076
C_f (1D)	0.0026	0.0020	0.0019	0.0019
ST (N)	3379	3342	3353	3183
ρ (kg/m^3)	1.005	0.609	0.416	0.292
V (m/s)	1058	1385	1701	1989
M	2.08	2.57	3.02	3.32
P_t (kPa)	1701	2607	4127	5458
P (kPa)	190.3	130.4	97.75	78.17
T_t (K)	1159	1573	2030	2549
T(K)	660	747	818	931
γ	1.369	1.360	1.352	1.341
C_p (J/kg-K)	1064	1085	1103	1128
η_{KE}	0.8964	0.9046	0.9039	0.8991
η_{KE} (adiabatic)	0.9663	0.9582	0.9585	0.9555
Total Pressure Recovery	0.535	0.398	0.307	0.214

instrumentation plan for these sections. In these images, wall pressure contours from the Mach 5 simulations are shown.

SUMMARY

Results for the HF2 revised forebody design have been presented. The calculations were performed across a nominal dynamic pressure trajectory. Basic flow features, surface quantities, inflow

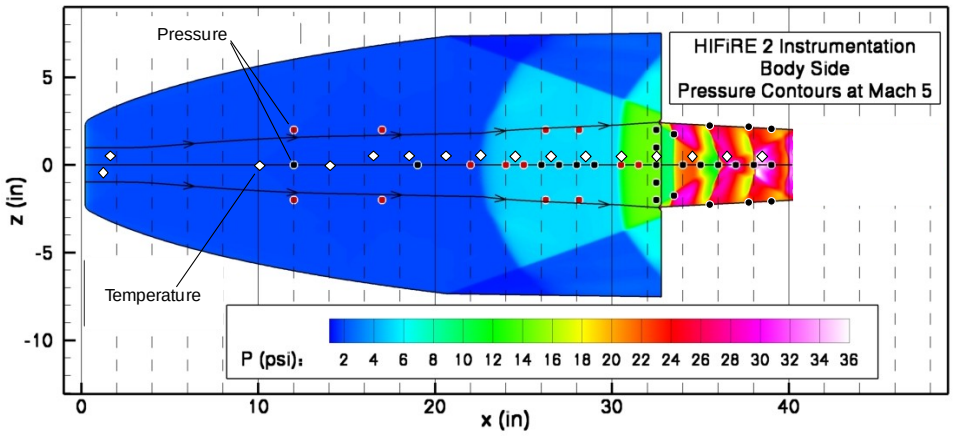

(a) Body instrumentation.

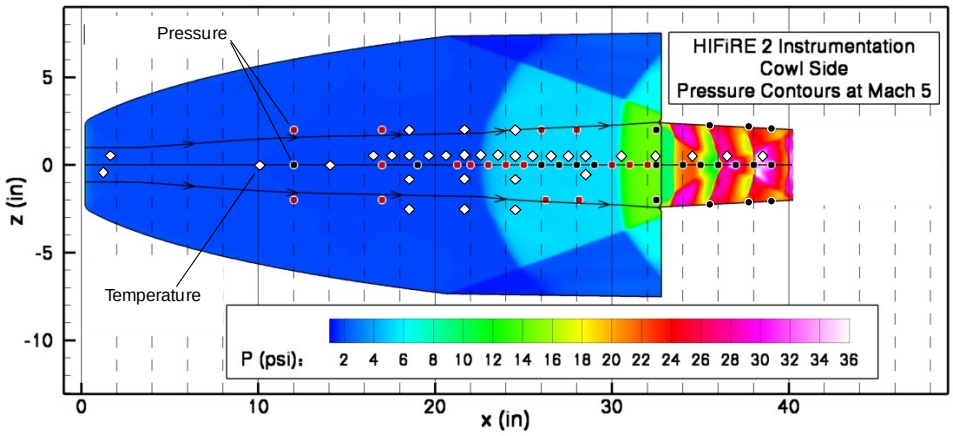

(b) Cowl instrumentation.

Figure 5. Forebody/inlet instrumentation plan.

planes for fueled combustor analysis, and a revised mass capture schedule were included. The modified forebody design meets all project requirements except the original Mach 8.5, q = 1000 psf combustor entrance 1D static pressure requirement. Despite this, the modified design allowed significant payload weight and length reduction. It also enabled the updated shroud requirements to be consistent with the previous experience base of the shroud manufacturer.

ISOLATOR/COMBUSTOR DESIGN MODIFICATIONS

The baseline geometry of the isolator/combustor section[5] was not influenced by the design modifications to the forebody. Table 5 and Figure 6 show flowpath coordinates (relative to the isolator entrance station) and a schematic of the isolator/combustor flowpath, respectively. The fuel injector diameters, however, were scaled in response to the reduction in air mass capture. The description that follows presents the approach used to scale the fuel injector diameters. Also presented is the revised instrumentation plan for the isolator/combustor sections.

Table 5. Isolator/combustor geometry.

Station	x (inches)	y (inches)
1	0.000	±0.500
2	8.000	±0.500
3	11.596	±0.582
4	11.581	±1.256
5	14.150	±1.315
6	15.794	±0.677
7	28.003	±0.954
P1	9.596	±0.536
S1	16.500	±0.693

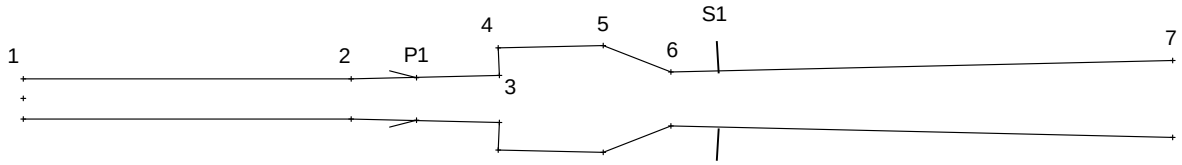

Figure 6. Baseline isolator/combustor flowpath schematic.

FUEL INJECTOR DIAMETER SCALING

Assuming the combustor will be operated on the same ϕ-schedule that was prescribed with the original forebody, the fuel flow rate will be adjusted based on the revised air mass capture:

$$\frac{W_{f,9}}{W_{f,12}} = \frac{\phi \cdot (f/a)_{ST} \cdot W_{air,9}}{\phi \cdot (f/a)_{ST} \cdot W_{air,12}} = \frac{W_{air,9}}{W_{air,12}}$$

The fuel flow rate ratio is also related to the fuel injector geometry by:

$$\frac{W_{f,9}}{W_{f,12}} = \frac{(\rho VAC_d)_{f,9}}{(\rho VAC_d)_{f,12}}$$

Assuming that the fuel injectors are choked, have the same physical characteristics (i.e., discharge coefficient), and that the static fuel properties (P and T) at injection are the same for the two forebody capture heights, then:

$$\frac{W_{f,9}}{W_{f,12}} = \frac{(A)_{f,9}}{(A)_{f,12}} = \frac{d_{f,9}^2}{d_{f,12}^2}$$

Thus, the new injector diameter is directly related to the square-root of the ratio of captured mass flow rates. In this resizing approach, the fuel momentum flux will be the same for the original and resized injectors because the fuel properties (P and T) were assumed to be constant and the injectors were assumed to be choked. The results of this resizing approach are given in Table 6 for both P1 and S1 injectors. It should be noted that the fuel injection angles remain as prescribed in the baseline design (P1 is 15-deg. relative to the wall, S1 is 90-deg. relative to the wall).

The air stream momentum flux decreases for the revised forebody. Thus, the fuel-to-air momentum flux ratio in this resizing approach increases slightly (approximately 20 – 25%). Also, because the fuel pressure was assumed to be constant and the combustor static pressure decreases for the revised forebody, the smaller fuel injectors are more likely to be choked across the range of Mach numbers expected in flight.

ISOLATOR/COMBUSTOR INSTRUMENTATION PLAN

A total of 156 pressure taps and 38 thermocouples are planned to be integrated into the isolator and combustor sections. Six of these pressure taps are dedicated to making measurements with high frequency response. The majority of the pressure taps are positioned on the spanwise centerline of the flowpath, although off-centerline measurements will be made at several axial stations. In particular, more dense arrays of pressure measurements are made at the isolator entrance, combustor exit, and two stations near the primary fuel injection

Table 6. Injector sizing results.

M	6	7	8	
q (psf)	1817	1730	1600	
$W_{air,9}$ / $W_{air,12}$	0.804	0.796	0.785	
$d_{f,9}$ / $d_{f,12}$	0.897	0.892	0.886	
				Std Drill
$P1_9$ (inch)	0.112	0.111	0.111	**0.110**
$S1_9$ (inch)	0.084	0.084	0.083	**0.082**

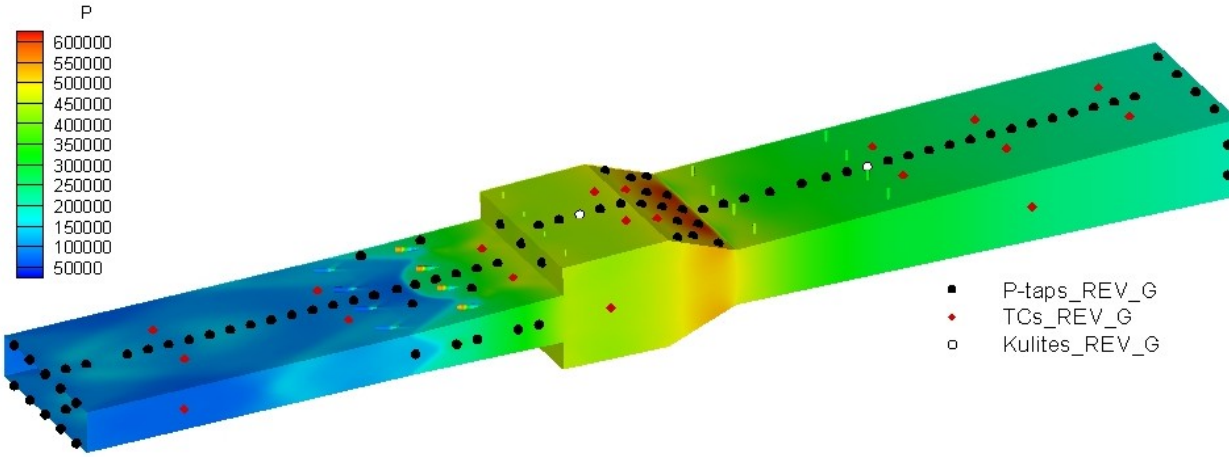

(a) Body and port sides.

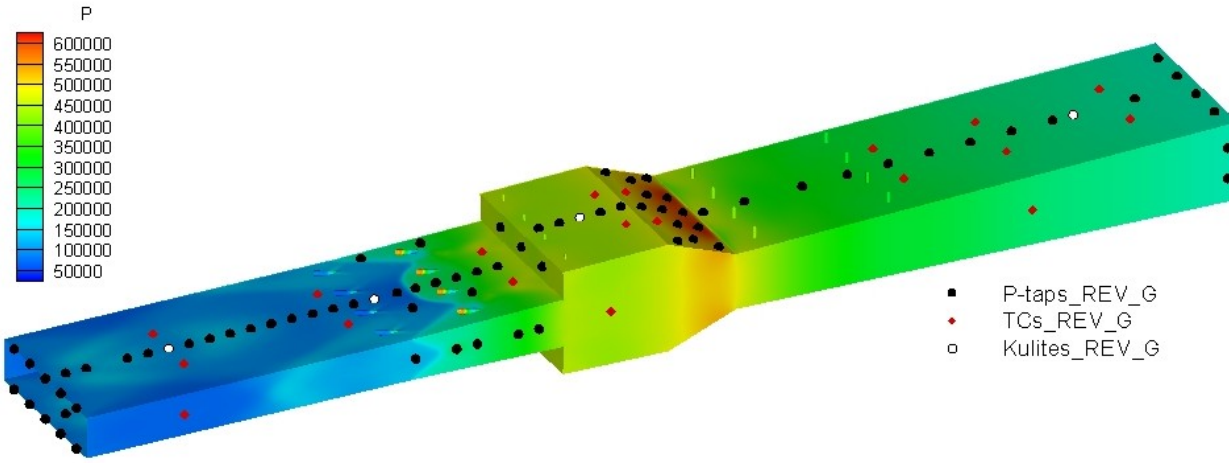

(b) Cowl and starboard sides.

Figure 7. Isolator/combustor instrumentation plan.

location. The cavity ramp region is densely instrumented in an attempt to resolve its contribution to the total wall pressure force.[6] Wall temperatures are included at various locations in an attempt to monitor flowpath health and to determine heat loss during the various phases of the experiment. Sparse measurements are also included on the port and starboard side walls of the flowpath. Figure 7 illustrates the current instrumentation plan for these sections. Black symbols represent static pressure taps, red symbols indicate thermocouples, and white symbols correspond to high-speed pressure measurements. In these images, wall pressure contours from Mach 8 numerical simulations are shown.

SUMMARY

The fuel injectors were resized as a result of the forebody design change. The resulting injector diameters were reduced in response to the air mass capture reduction. Other features of the isolator/combustor flowpath were not adjusted. The flowpath instrumentation plan includes wall pressure (both low and high frequency response) and temperature measurements.

NOZZLE DESIGN MODIFICATIONS

As a result of the modified forebody, changes were made to the initial HIFiRE Flight 2 nozzle design (N1) to meet system payload requirements[1] (system illustrated in Figure 8). The new design (N2) is 9.84 inches shorter than the N1 nozzle and extends to the new 17.58-inch payload diameter at the 77.4-inch axial station. The smaller N2 design helps meet the payload system requirement for a lighter payload. A new cover design was added to the N2 design to shield the flowpath during boost. The new design meets payload system requirements without changing the basic design of the nozzle and flow characteristics. The instrumentation plan was updated to accommodate the new design. A total of 78 and 21 pressure taps and thermocouples respectively are planned to be installed in the N2 nozzle.

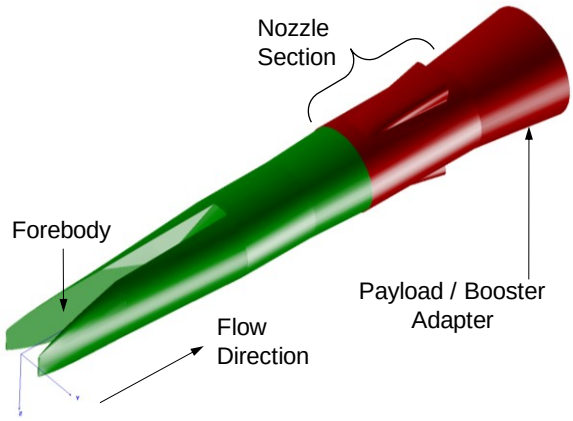

Figure 8. HF2 payload system.

NOZZLE DESIGN EVOLUTION

The evolution from the original nozzle design (N1) to the latest nozzle design (N2) integrated with the flowpath covers is shown in Figure 9. The N1 nozzle was originally designed to minimize the influence of the nozzle on the combustor without any concern for performance. This was achieved by placing the nozzle centerbody as far aft as possible from the nozzle entrance. The resulting bow shock exits the nozzle without impinging on the sidewall of the nozzle. This reduces the likelihood of any separations occurring in the nozzle section due to shock/boundary layer interactions. The original nozzle extended out to a 22-inch payload diameter. The payload diameter was reduced to 17.58-inches at the 77.4-inch axial station. This reduction resulted from requirements to reduce the weight of the payload. The nozzle was also reduced in length and diameter to accommodate the new payload diameter and further reduce the payload weight. The latest design (N2) maintained the flow characteristics and overall shape as the original N1 design. Flowpath shielding was added after the N2 design was completed as result of new requirements to protect the flowpath during boost before shroud separation. The final conceptual design is seen in Figure 9. The cover is a smooth ten degree wedge which is blended with the payload airframe. The cover begins as a circle shape and then blends into a hyperbolic shape at the end of the cover.[7] The final picture in the

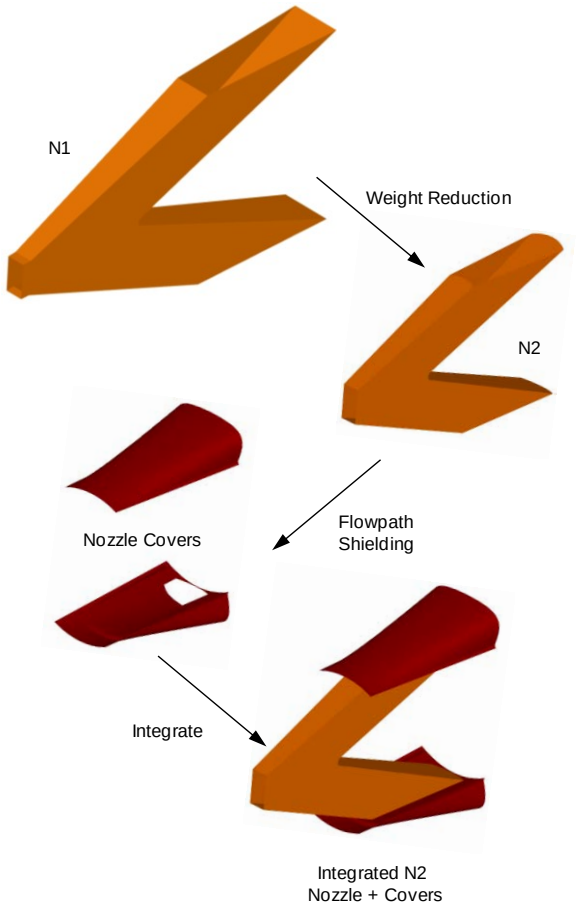

Figure 9. Nozzle and cover design evolution.

bottom right corner of Figure 9 shows the integrated N2 nozzle and cover designs.

A comparison of the N1 and N2 nozzle is provided in Figure 10. This illustrates the significant reduction in diameter and length of the nozzle. A reduction of 5.04-inches was first achieved simply due to the change in outer payload diameter. The nozzle sidewall was shifted forward by one inch. A larger gap between the nozzle sidewall and the centerbody shock resulted because of the reduction in outer diameter. With this larger gap and the movement of the sidewall forward allowed for the centerbody to be moved forward 4.44-inches while preserving the flow characteristics of the N1 nozzle. A total reduction of 9.84-inches in length was achieved. The weight of the payload is directly proportional to the length assuming constant diameter sections. This represents a significant weight reduction considering that the nozzle original length was approximately 40-inches.

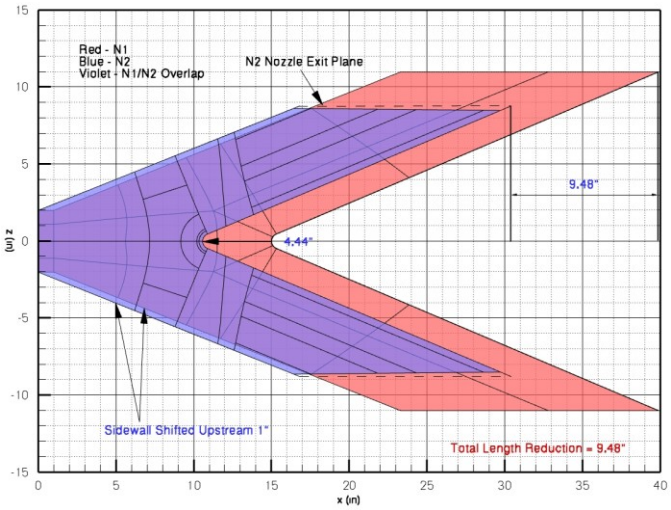

Figure 10. N1 and N2 design comparison.

N2 NOZZLE COVER CHARACTERISTIC DIMENSIONS

Table 7 provides the wetted surface area of the N2 nozzle cover (1/4 model). The largest surfaces are the cowl wall, cover inner, and cover outer surfaces. The smallest surfaces are the centerbody surfaces and the nozzle sidewalls. The characteristic dimensions of the N2 nozzle are provided in Table 8. The overall dimensions for length, height, and width are 30.5-, 24.0-, and 9.31-inches respectively. The cross-sectional area for the three nozzle sections is given in Figure 11. Discontinuous changes in cross-sectional area occur at the bifurcation point at 79-inches and at the start of the cover section at 84-inches. The cross-sectional area at the cover exit is more than 7 times larger than the cross-sectional area at the nozzle entrance.

FLOW CHARACTERISTICS

As discussed in the previous sections, the flow characteristics of the N2 nozzle preserved the flow characteristics of the N1 nozzle. The flow characteristics can be seen in Figure 12 with Mach number contours at the symmetry plane of the nozzle. The flow expands in the nozzle section then bifurcates at the nozzle centerbody. A bow shock is produced at the centerbody leading edge and exit through the nozzle exhaust ducts. The bow shock then impinges on the nozzle cover and the flow is turned 12 degrees back toward the booster. The exhaust gases expand in the cover section forming a vortex at the sides of the cover (see Figure 13). Finally the flow exits the nozzle cover and interacts with the freestream flow. Over the Mach number range from 6 to 8

Table 7. Surface wetted area (1/4 model).

	Description	A (in^2)
1	Cowl Side Wall	166.61
2	Centerbody Leading Edge	0.84
3	Centerbody Port	38.92
4	Port Sidewall	23.71
5	Cover Inner Surface Closeout	1.38
6	Airframe	29.89
7	Cover Inner Surface	87.53
8	Cover Outer Surface	97.04
9	Backstep	0.82

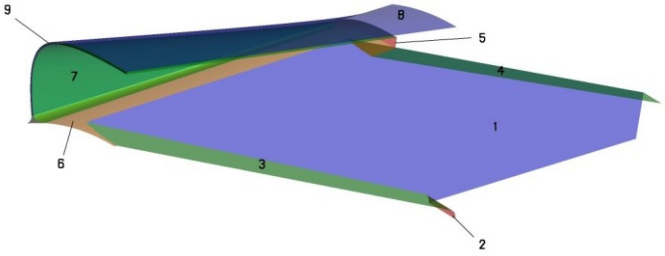

and from tare to fueled conditions no significant changes in the flow character was observed. The centerbody bow shock location was fairly insensitive over this range of conditions.

NOZZLE INSTRUMENTATION PLAN

A total of 78 pressure taps and 21 thermocouples are planned to be added to the nozzle section. No instrumentation is currently planned to be installed on the nozzle cover. The majority of the instrumentation in the nozzle uses nozzle symmetry to acquire sufficient resolution of flow gradients such as the nozzle flow expansion observed at the nozzle entrance. Additional instrumentation was added to measure the location of flow features such as the location of the centerbody bow shock and sidewall separation at the centerbody leading edge. See Figure 14 for the pressure and thermocouple locations on the body and cowl sides of the nozzle. A flood contour is used for pressure and contour lines are used for heat flux. The pressure taps have enough resolution to capture the flow expansion at the nozzle entrance and map out the centerbody bow shock location. The thermocouples are placed in key locations to measure peak thermal loads (as seen in Figure 14). Instrumentation is placed on the nozzle centerbody leading edge to measure peak pressure and thermal loads at the location of a shock/shock interaction and impingement on the centerbody leading edge.

SUMMARY

The latest N2 design meets payload requirements to reduce weight. Flowpath covers were added to protect the flowpath during boost. The N2 nozzle operates as the previous N1 nozzle and no adverse effects were observed from the addition of the nozzle covers over the desired HF2 experimental range. The instrumentation plan was updated to accommodate the N2 geometry changes. No instrumentation is planned to be installed on the flowpath covers.

Table 8. N2 characteristic dimensions.

Characteristic Dimension	Value
Overall Length (nozzle + cover)	30.50”
Overall Width (Y-axis)	9.31”
Overall Height (Z-axis)	24.00”
Nozzle Body/Cowl Angle	2.50°
Nozzle Port/Starboard Angle	22.00°
Centerbody Port/Starboard Angle	23.12°
Payload Outer Diameter	17.58”
Nozzle Start	68.44”
Nozzle End	98.12”
Internal Cover Start	84.00”
External Cover Start	80.74”
Cover End	98.94”
Cover Wedge Angle	10.00°
Centerbody Leading Edge Radius	0.5”

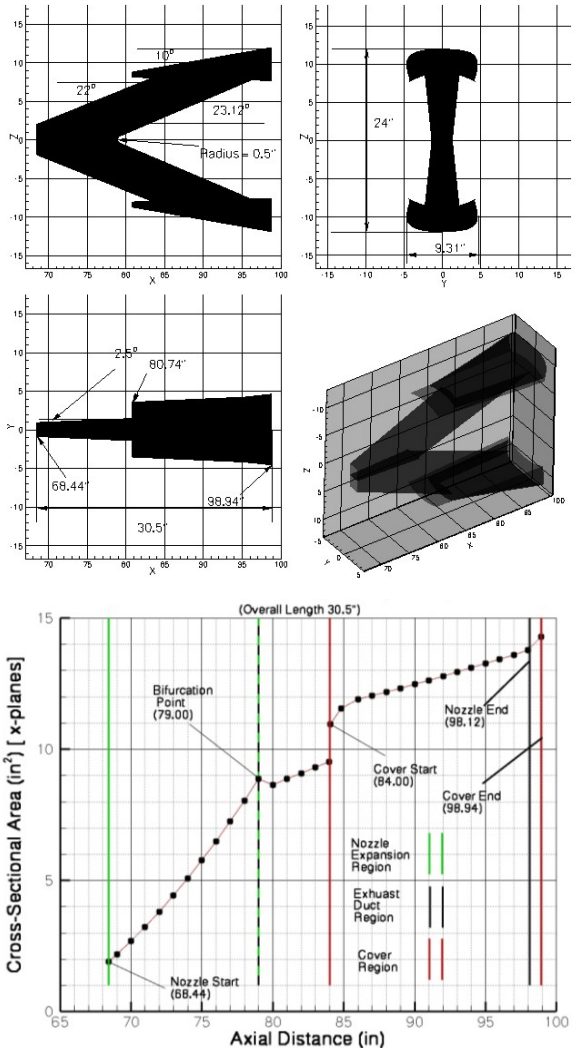

Figure 11. N2 cross-sectional area (1/4 model).

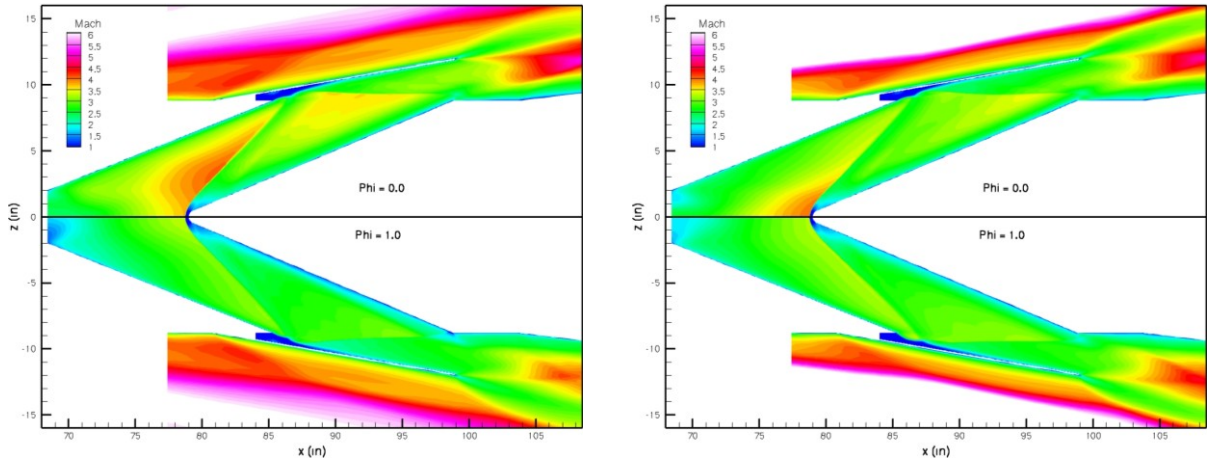

(a) Mach 6. (b) Mach 8.

Figure 12. Symmetry plane Mach number contours at nominal dynamic pressure and wall temperature of 800 K.

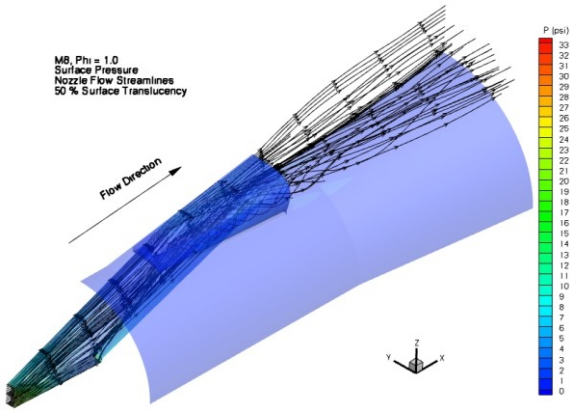

Figure 13. Nozzle flow stream lines and surface pressure (nominal q).

SUMMARY

The HIFiRE Flight 2 experiment offers a unique opportunity to study mode transition and supersonic combustion performance using a surrogate hydrocarbon fuel over a Mach number range from 5.5 to 8+. This experiment involves a flight trajectory based on current sounding rocket capabilities and a novel second-stage ignition approach that achieves a nearly constant flight dynamic pressure over this range of Mach numbers. The captive-carry scramjet flowpath will be heavily instrumented, using both conventional wall instrumentation and in-stream optical diagnostics, in order to adequately assess the operability and performance of the device as well as verify the tools used for its design. As the overall payload system design has matured, changes to the flowpath were required in order to reduce the overall weight and to meet shroud design requirements. The forebody capture height was reduced from 12- to 9-inches, thereby allowing the forebody to be made substantially smaller (length, diameter, and therefore weight) without compromising experimental requirements. The reduced mass capture necessitated a change to the fuel injector diameters, but no additional changes to the isolator/combustor flowpath. The nozzle design was modified to adapt to the new smaller overall payload diameter resulting in additional weight and length savings. In addition, stationary covers were added to the external portion of the nozzle in order to protect the scramjet nozzle exit regions during the boost phase of the trajectory. The instrumentation plan was updated as a result of these design modifications

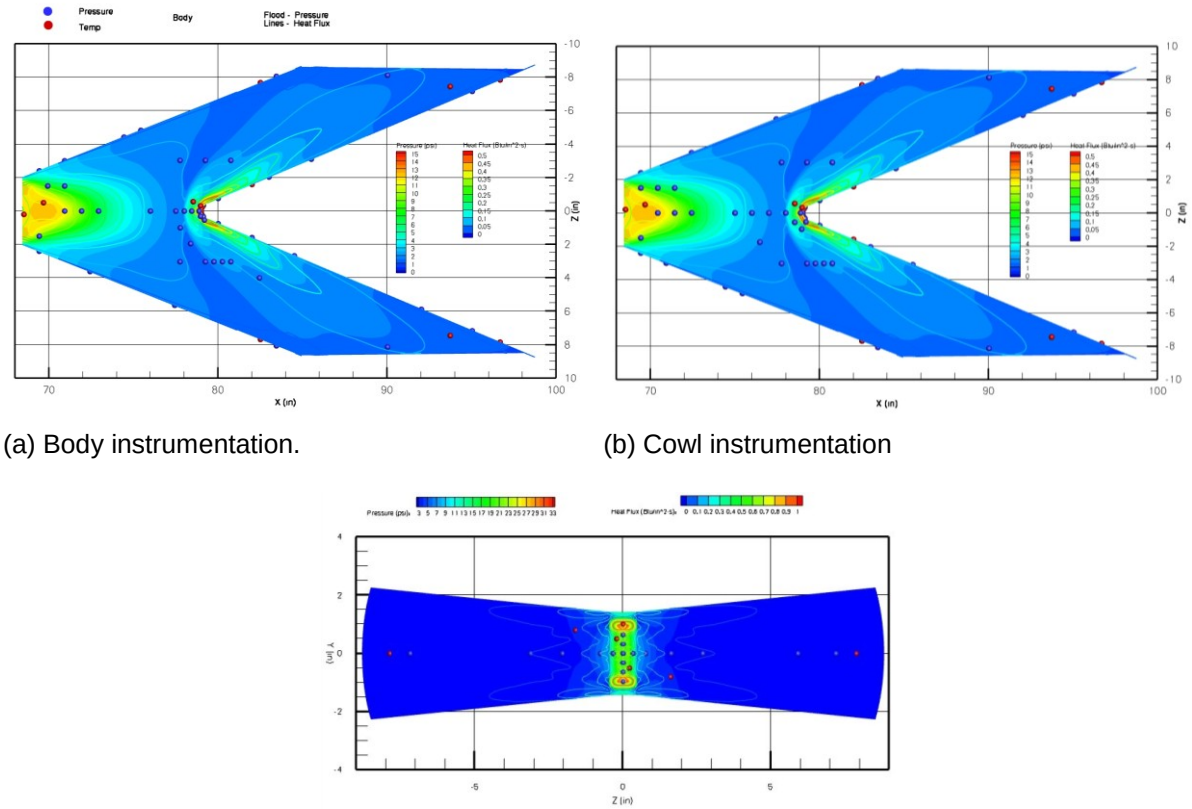

(a) Body instrumentation.

(b) Cowl instrumentation

(c) Centerbody instrumentation.

Figure 14. Nozzle instrumentation plan.

REFERENCES

[1] Jackson, K. R., Gruber, M. R., Jackson, T. A., and Hass, N. E., "HIFiRE Flight 2 Scramjet Flight Experiment Overview," JANNAF Propulsion Meeting, Newton, MA, May 12-16, 2008.

[2]Ferlemann, P.G., "Forebody and Inlet Design for the HIFiRE 2 Flight Test," JANNAF Propulsion Meeting, Newton, MA, May 12-16, 2008.

[3]Kantrowitz, A., and Donaldson, C., "Preliminary Investigation of Supersonic Diffuser," NACA WRL-713, 1945.

[4]VULCAN home page, http://vulcan-cfd.larc.nasa.gov.

[5] Gruber, M., Jackson, K., Jackson, T., and Liu, J., "Hydrocarbon Fueled Scramjet Flowpath Development for Mach 6-8 HIFiRE Flight Experiments," JANNAF Propulsion Meeting, Newton, MA, May 12-16, 2008.

[6] Gruber, M., Barhorst, T., Jackson, K., Eklund, D., Hass, N., Storch, A. M., and Liu, J., "Instrumentation and Performance Analysis Plans for the HIFiRE Flight 2 Experiment," AIAA Paper 2009-5032, August 2009.

[7]McDaniel, K., "HIFiRE Flight 2 Nozzle Design 2 Geometry Description (With Ten Degree Cover)," HF2-TN-007, 26 March 2009.